

# NEW HIGH POWER LINACS AND BEAM PHYSICS\*

T.P.Wangler, E.R.Gray, and S.Nath, Los Alamos National Laboratory, Los Alamos, NM, 87545, K.R.Crandall, Amparo Corporation, Santa Fe, NM 87504, and K. Hasegawa, Japan Atomic Energy Research Institute, Tokai-mura, Ibaraki-ken 319-11, Japan.

## Abstract

New high-power proton linacs must be designed to control beam loss, which can lead to radioactivation of the accelerator. The threat of beam loss is increased significantly by the formation of beam halo. Numerical simulation studies have identified the space-charge interactions, especially those that occur in rms mismatched beams, as a major concern for halo growth. The maximum-amplitude predictions of the simulation codes must be subjected to independent tests to confirm the validity of the results. Consequently, we compare predictions from the particle-core halo models with computer simulations to test our understanding of the halo mechanisms that are incorporated in the computer codes. We present and discuss scaling laws that provide guidance for high-power linac design.

## 1 OVERVIEW

High-intensity, high-energy proton linacs are being designed for new projects around the world [1]. Typical requirements for these linacs include high peak current (beam current averaged over an rf period) near 100 mA, corresponding to about  $10^9$  particles per bunch at bunch frequencies of several hundred MHz, and final energies near 1 GeV. An important design objective is to restrict beam losses to levels that will allow hands-on maintenance throughout the linac. If one adopts a hands-on-maintenance criterion that limits the activation level to 20 mRem/hr at a distance of 1 m from a copper accelerating structure an hour after shutdown of the accelerator, the maximum tolerable beam-loss rate can be estimated from calculations reported in Ref. [2]. If the beam-loss rate is expressed in terms of the lost beam power, the loss rate above 100 MeV must be limited to several tenths of a beam-Watt per meter. The LANSCE proton linac, which operates with hands-on maintenance at the 17-mA peak and 1-mA average current levels, achieves typical beam-loss rates above 100 MeV of less than a few tenths of a Watt per meter. The challenge for the new generation of linacs is to provide larger average currents without increasing the beam loss.

Numerical simulation codes with a space-charge calculation based on solving Poisson's equation,

provide a practical method of self-consistent calculations for so-called collisionless beams that satisfy Liouville's theorem. Liouville's theorem would be violated in beams that are affected significantly by particle collisions. However, the beam spends only a short time in the linac, typically several microseconds, and one finds that intrabeam scattering [3], resulting from multiple Coulomb collisions, and the Touschek effect [4], resulting from single Coulomb collisions, are small effects compared with the space-charge forces.

Numerical-simulation studies predict that a major threat of beam loss in the new generation of high power linacs is associated with halo induced by beam mismatch [5]. Because there is not a consensus about its definition, halo remains an imprecise term. In any given computer simulation one can unambiguously define an rms beam size, and a maximum particle displacement. Provided that the statistical precision is sufficiently adequate that the results are not sensitive to the motion of a few lone outer particles, the ratio of the maximum displacement to the rms size of the matched beam, which we call the maximum to rms ratio, is a useful figure of merit. Qualitatively, one can describe the evolution of the outer regions of the particle distribution for the case of an initial compact particle distribution (excluding the singular K-V distribution). A compact particle distribution might be arbitrarily defined as having initial position and velocity coordinates that are contained within about  $3\sigma$ . If this beam evolves in an rms-matched state, an equilibrium distribution develops in which the density at the beam edge falls off within about a Debye length. The Debye tail, whose size is a function of both the rms emittance and beam current, is a consequence of the propensity of the charges in a beam to provide shielding within the beam core. Rms emittance growth and associated growth of the Debye tail can occur, especially through longitudinal-transverse coupling of the space-charge force [6]. For a beam with a given current and emittance, the size of this tail relative to the rms size can be changed by changing the focusing strength. Although there is no consensus about whether to call the Debye tail a halo, values of the maximum to rms ratio larger than about 5 are generally not observed in simulations, and the beam retains a very compact distribution [7].

---

\* Work supported by US Department of Energy

The outer region for a beam, with the same initial compact particle distribution in an rms mismatched state, evolves differently. Many theoretical and numerical studies of halo formation in mismatched beams have been reported, showing larger amplitudes extending well beyond the Debye-tail of a matched beam. For practical estimates of expected mismatch in linacs, values for the maximum to rms ratio as large as 10 to 12 have been observed in simulations, and it is generally agreed that this is called halo. Particle-core models for both a cylindrical beam [8] and a spherical bunch [9] provide quantitative predictions for the amplitudes. In these models the space-charge field from a beam core, oscillating radially in the symmetric breathing mode in a uniform linear-focusing channel, is represented by a hard-edged, spatially-uniform density distribution. The breathing mode appears to produce the largest amplitudes seen in simulations. The amplitude of the breathing-mode oscillation is directly related to the magnitude of the initial rms mismatch of the beam. The behavior of halo particles is studied in the model by representing them with single particles that oscillate through the core and interact with it. The particles slowly gain or lose energy as a result of multiple traversals through the core. A parametric resonance exists [10] when the particle frequency is half the core frequency. The amplitude growth for the resonant particles is self limiting, because outside the core, the net restoring force increases with radius, which produces a dependence of frequency on the particle amplitude; thus the resonant condition is restricted to a range of particle amplitudes. Chaos, which may increase the halo population, is observed at low tune-depression ratios [11].

By numerically integrating the trajectories from the models, the maximum amplitudes have been calculated as a function of an initial mismatch parameter  $\mu$ , the ratio of the initial rms core size to the matched rms core size. The normalized maximum particle amplitude is described over a useful range of tune-depression ratios by an approximate empirical formula

$$x_{\max} / a = A + B|\ln(\mu)|, \quad (1)$$

where  $x_{\max}$  is the maximum resonant-particle amplitude,  $a$  is the matched rms core size, and  $A$  and  $B$  are weak functions of the tune-depression ratio, given in Ref. [9]. Approximate values for the cylindrical beam are  $A \cong B \cong 4$ , and for the spherical bunch,  $A \cong B \cong 5$ . Equation 1 is not a good approximation for values of  $\mu$  very near 1, where  $x_{\max}/a$  rapidly approaches 2 for the continuous beam, and  $\sqrt{5}$  for the spherical bunch.

For the spherical bunch geometry, we expect that both the transverse and the longitudinal halo are driven primarily by the breathing mode. In the limit of a prolate spheroid or cigar-shaped bunch with a large aspect ratio, the transverse motion is still dominated by the breathing mode. Then, the longitudinal motion is dominated by the lower-frequency antisymmetric mode [12] in which the radial and longitudinal displacements are out of phase.

## 2 SCALING OF EMITTANCE GROWTH AND HALO

Assuming that the bunch can be modeled as a long cylinder with a uniform longitudinal profile, we obtain simple scaling formulas for transverse rms emittance growth and maximum particle amplitude for the mismatched beam. It is known that the space-charge-induced rms-emittance growth is a function of the tune depression ratio  $k/k_0$ , where  $k$  and  $k_0$  are the transverse phase advances per unit length, with and without space charge. For a long cylindrical bunch where end effects can be ignored, and assuming uniform transverse focusing, the rms emittance-growth ratio is a function of the tune depression ratio. In the smooth approximation, where the focusing is represented by an equivalent uniform focusing channel, we may write  $k/k_0 = \sqrt{1+u_t^2} - u_t$ , where  $u_t$  is a space-charge parameter given by

$$u_t = \left( \frac{qI}{16\pi\epsilon_0\ell f\gamma^2} \right) \left( \frac{1}{mc^2\beta} \right) \left( \frac{1}{\epsilon_n k_0} \right). \quad (2)$$

The parameters appearing in the Eq.(2) are the charge  $q$ , rest energy  $mc^2$ , average beam current  $I$ , effective bunch length  $\ell$ , bunch frequency  $f$ , relativistic mass factor  $\gamma$ , velocity (relative to that of light)  $\beta$ , and normalized rms emittance  $\epsilon_n$ . The average current is related to the number of particles per bunch  $N$  and the bunch frequency, by  $I=qNf$ .

The particle-core model for an rms-mismatched beam predicts that the halo particles created by the resonance have a maximum amplitude for a given core-oscillation amplitude. From Eq.(1), the numerical solution predicts that the maximum amplitude is proportional to the matched rms size  $a$  of the core, given by

$$a^2 = \frac{\epsilon_n}{k_0 B \gamma} \left[ \sqrt{1+u_t^2} + u_t \right]. \quad (3)$$

In the space-charge dominated limit, when  $u_t \gg 1$ , the rms beam size is

$$a^2 \cong \frac{2\varepsilon_n u_t}{k_0 \beta \gamma} = \left( \frac{qI}{8\pi\varepsilon_0 \ell f \gamma^2} \right) \left( \frac{1}{mc^2 \gamma \beta^2} \right) \frac{1}{k_0^2}, \quad (4)$$

which is independent of the emittance. The emittance-dominated limit corresponds to  $u_t \ll 1$ , and we find

$$a^2 \cong \frac{\varepsilon_n}{k_0 \beta \gamma} \left[ 1 + \left( \frac{qI}{16\pi\varepsilon_0 \ell f \gamma^2} \right) \left( \frac{1}{mc^2 \beta} \right) \left( \frac{1}{\varepsilon_n k_0} \right) \right]. \quad (5)$$

In Eq.(5), the second term is much less than unity, and smaller emittance results in smaller  $a$  and smaller maximum amplitude.

In spite of these scaling results, which show that the maximum amplitude for an rms mismatched beam decreases with increased focusing strength (larger  $k_0$ ), a consensus does not exist that the strongest transverse focusing yields the optimum solution. First, there is a concern that if the transverse focusing is too strong, the longitudinal space-charge forces will increase and longitudinal halo may become a problem. Then, related to this concern, some argue [13,14] that even at high energies the focusing strengths should be chosen to maintain equipartitioning between all three planes, to prevent the possibility of any energy exchange. If the linac frequency and accelerating gradient are fixed, one finds that because of the reduction in the longitudinal focusing strength with increasing energy, equipartitioning requires that the transverse focusing must also be weakened. This shifts the beam towards a more transverse-space-charge dominated regime, so that, although there is a shorter Debye tail for a matched or nearly matched beam [15], one finds both a larger transverse rms size and larger maximum amplitude [16]. Until some of these questions are resolved, it is prudent to require sufficient adjustability in the electromagnetic-quadrupole focusing to allow an experimental optimization.

### 3 HALO SIMULATION TESTS

As a test of the capabilities of the space-charge codes to calculate the maximum particle amplitudes, numerical simulation runs were carried out for four different cases using  $10^4$  particles per run, as summarized in Table 1. Two space-charge codes were used, one based on Gauss' law, and the other is SCHEFF, which is based on a 2-D ( $r$ - $z$ ) particle-in-cell method [17]. Several initial distributions were used, including Gaussian in both position and velocity space (truncated at  $3\sigma$ ), semi-Gaussian (uniform in space and Gaussian in velocity space), and Waterbag (uniformly-filled ellipsoid in 4-D or 6-D phase space). For each case there is a set of runs for different values of the

initial mismatch parameter  $\mu$ , which is the same in all planes. After the beam sizes were set for a given mismatch parameter, the velocities were scaled to make the emittance the same as for the matched case.

**Table 1. Simulation runs for Comparison with the Particle-Core Models.**

Fig.	Space-Charge Code	Particle-Core Model	Focusing Channel
1	Gauss	Cylinder	Uniform
2	Gauss and SCHEFF	Cylinder	Uniform
3	Gauss	Sphere	Uniform
4	SCHEFF	Sphere	FODO

Figs. 1 through 4 show the ratio of the maximum particle amplitude from simulation to the rms size of the matched beam, versus the mismatch parameter  $\mu$ . For Figs. 1, 3, and 4, two curves are shown from the appropriate particle-core model, showing the ratio of the maximum resonant-particle amplitude to the rms size of the matched core. The lower and upper curves are for tune-depression ratios of 0.5 and 0.9. In Fig. 4, the points correspond to a maximum displacement and rms size that are averaged over the lattice period. The simulations for the uniform channels were run for at least 100 plasma periods, sufficient for the amplitudes to reach an apparent asymptotic value. A typical high-power linac may contain a few hundred plasma periods.

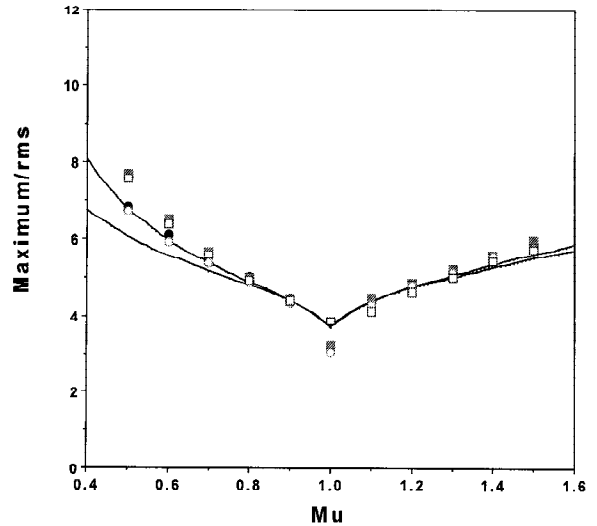


Fig. 1. Cylindrical-beam simulations comparing the particle core-model with the Gauss'-law space-charge code for a uniform-focusing channel. The solid and open symbols are for the initial Gaussian and Semi-Gaussian distributions, and the circles and squares are for tune-depression ratios of 0.5 and 0.9.

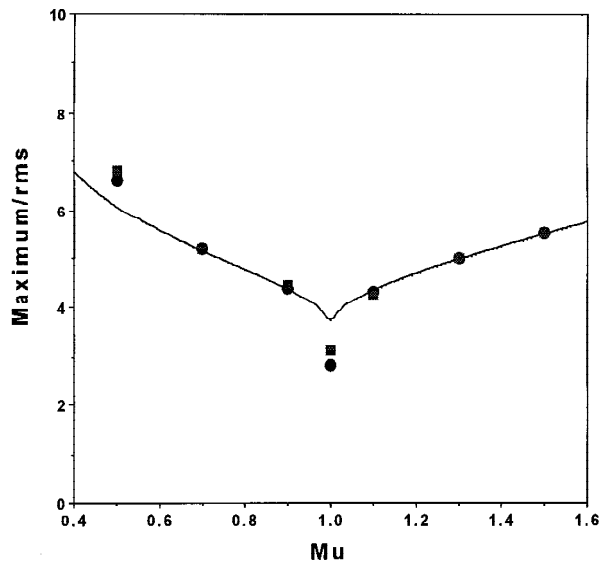


Fig. 2. Cylindrical-beam simulations comparing the cylinder particle core-model with the Gauss (circles) and SCHEFF (squares) space-charge codes for a uniform focusing channel, both for a tune-depression ratio of 0.5. The initial distribution is a 4-D Waterbag.

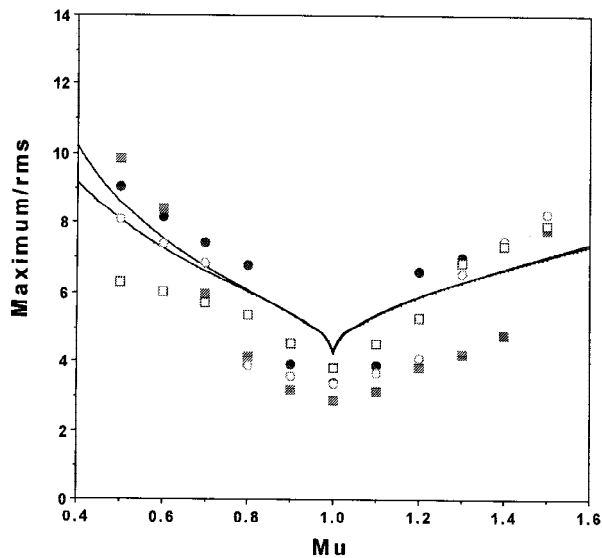


Fig. 3. Spherical-bunch simulations comparing the Gauss' law space-charge code with the sphere particle core-model for a uniform focusing channel. The solid and open symbols are for the initial Waterbag and Semi-Gaussian distributions, and the circles and squares are for tune-depression ratios of 0.5 and 0.9.

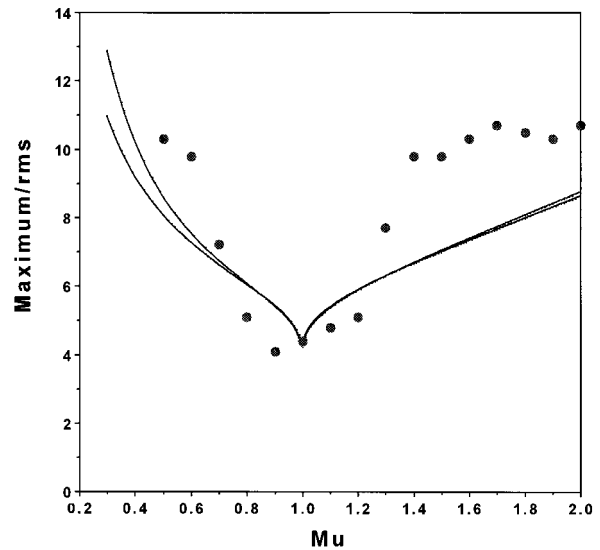


Fig. 4. Simulations comparing the SCHEFF space-charge code with the spherical particle core-model for a 7- to 217-MeV proton linac with 100-mA beam current, and FODO quadrupole-focusing with a variable tune-depression ratio. The initial distribution is a 6-D Waterbag, and the bunches have a variable prolate-spheroid geometry.

The agreement of the maximum amplitudes from the models and the Gauss'-law simulations for the uniform channel in Fig. 1 is remarkably good for both the initial Gaussian and semi-Gaussian distributions. In Fig. 2 the test is extended to the 4-D Waterbag distribution, comparing both the Gauss'-law and the SCHEFF simulation results. Although the details of the maximum amplitude trajectories for the Gauss'-law and the SCHEFF simulations were not exactly the same, the maximum amplitudes agree very well with each other and with the cylinder particle-core model. We consider this result an important initial test of the capability of the SCHEFF code. In Fig. 3, the Gauss'-law simulation for the spherical bunch shows a tendency for some points, especially with  $\mu$  values near 1, to remain below the curves of the particle-core models. These results suggest that halos may have more difficulty developing from some initial spherical-bunch states. Fig. 4, representing a simulation of a real linac, shows that the SCHEFF results for the larger mismatches (greater deviations from  $\mu=1$ ) are systematically higher than the sphere model by as much as 30%. Deviation of the points from the curves may be caused by inadequacies of either the model, or the SCHEFF space-charge calculations. For the linac simulation, we conclude that the results are consistent with the hypothesis that the breathing mode is the most important, although perhaps not the only driver of the beam halo produced by the simulation codes.

## 4 CONCLUSIONS

The particle-core models make quantitative predictions about the halo that is formed from the resonant interaction between individual particles and a mismatched-induced core oscillation in the breathing mode. The models predict that the halo will be limited to a maximum amplitude, which depends mostly on the magnitude of the initial mismatch. The simulation results, using two different space-charge codes, confirm the model predictions for the continuous beam in a uniform focusing channel. In other cases, discrepancies are observed, but the largest of these are only about 30%. We interpret the results to be consistent with the hypothesis that the breathing mode is the main source of the halo seen in the simulation codes. We believe that a reasonable estimate for the maximum mismatch-oscillation amplitude corresponds to values  $\mu$  that may deviate from unity by about 0.3 to 0.4.

We believe that a practical approach to beam-loss control is to inject a high-quality, well-collimated beam into the high-energy linac, and achieve minimal proton-beam loss at high energies by providing strong transverse focusing, carefully controlling the beam centroid, and providing large beam apertures. The optimal choice of transverse focusing strength will depend on the results of subsequent studies of longitudinal halo. Although we are acquiring a better understanding of the causes of beam halo in the simulation codes, and providing a better rationale for the aperture choice, it is prudent to provide a safety margin. Such a margin is necessary to allow for errors and for the possibility of physics effects, which are not treated or are inadequately treated in the present codes. Consequently, to further reduce the risk of high-energy beam loss, we believe that the design of a high-power proton linac can benefit from the use of large-aperture superconducting linacs at high energies, as is now proposed for APT.

## 5 ACKNOWLEDGMENTS

The authors acknowledge helpful discussions with R. Gluckstern, R. Ryne, J. Bernard, and S. Lund.

## REFERENCES

- [1] For a list of references to projects see M. Prome, "Major Projects for the Use of High-Power Linacs", Proc. of the XVIII Int. Linear Accel. Conf., 26-30 August, 1996, Geneva, Switzerland, CERN 96-07, 9.
- [2] A.P.Fetotov and B. Murin, Proc. of the 1976 Linear Accelerator Conf., Chalk River, Canada, p.377.
- [3] M. Reiser, "Theory and Design of Charged Particle Beams," John Wiley & Sons, Inc., New York, 1994. For a nonrelativistic formula that gives an upper limit, see Eq. 6.173 in Section 6.4.2 of the 1st Edition.
- [4] H. Bruck, "Circular Particle Accelerators, Institut National des Sciences et Techniques Nucleaires, Saclay, Presses Universitaires de France, 1966, Los Alamos Translation LA-TR-72-10 Rev. See Eq. 30-17, Chapter XXX.
- [5] A. Cucchetti, M. Reiser, and T. P. Wangler, Proc. 1991 Part. Accel. Conf., IEEE Cat. No. 91CH3038-7 (1991) 251.
- [6] M. Pabst and K. Bongardt, "Halo Simulation in a Realistic proton Linac Design, Proc. of the XVIII Int. Linear Accel. Conf., 26-30 August, 1996, Geneva, Switzerland, CERN 96-07, 9.
- [7] R.D.Ryne and T.P.Wangler, "Recent Results in Analysis and Simulation of Beam Halo", Int. Conf. on Accelerator-Driven Transmutation Technology and Applications, Las Vegas, NV, 1994, AIP Conf. Proc. 346, pp. 383-389.
- [8] J. S. O'Connell, T. P. Wangler, R. S. Mills, and K. R. Crandall, Proc. 1993 Part. Accel. Conf., Washington, DC(1993) 3657.
- [9] T.P. Wangler, R.W. Garnett, E.R.Gray, R.D.Ryne, and T.S.Wang, Dynamics of Beam Halo in Mismatched Beams, Proc. of the XVIII Int. Linear Accel. Conf., 26-30 August, 1996, Geneva, Switzerland, CERN 96-07, 372.
- [10] R. L. Gluckstern, Phys. Rev. Lett. 73(1994) 1247.
- [11] J. M. Lagniel, Nucl. Inst. Meth. A345(1994) 46; A345(1994) 405.
- [12] J. Barnard and S. Lund, these proceedings.
- [13] M. Reiser and M. Brown, "RF Linac Designs with Beams in Thermal Equilibrium", Space Charge Dominated Beams and Applications of High Brightness beams, Bloomington, IN, 1995, AIP Conf. Proc. 377, pp. 329-340.
- [14] R. A. Jameson, in Advanced Accelerator Concepts, AIP Conf. Proc. 279, (1993), p 969.
- [15] L.M. Young, "Equipartitioning in a High Current Proton Linac", these proceedings.
- [16] R.W.Garnett, "Linear Accelerator for Tritium Production", ref. 13, pp. 60-73.
- [17] K.R.Crandall, unpublished.